Aqueous microsolvation of CdCl 2 : Density functional theory and Born-Oppenheimer molecular dynamics studies

A. Ramirez-Solis, Laurent Maron

Aqueous microsolvation of $CdCl_2$: Density functional theory and Born-Oppenheimer molecular dynamics studies

A. Ramírez-Solís, and L. Maron

Citation: J. Chem. Phys. **141**, 094304 (2014); doi: 10.1063/1.4894286
View online: https://doi.org/10.1063/1.4894286
View Table of Contents: http://aip.scitation.org/toc/jcp/141/9
Published by the American Institute of Physics

Aqueous microsolvation of $CdCl_2$: Density functional theory and Born-Oppenheimer molecular dynamics studies

A. Ramírez-Solís[a] and L. Maron
Laboratoire de Physicochimie de Nano-Objets, INSA-IRSAMC, Université de Toulouse III, 135, Avenue de Rangueil, Toulouse, F31077, France

(Received 18 March 2014; accepted 18 August 2014; published online 3 September 2014)

We report a systematic study of aqueous microsolvation of $CdCl_2$. The optimized structures and binding energies of the $CdCl_2$-$(H_2O)_n$ clusters with $n = 1$–24 have been computed at the B3PW91/6-31G** level. The solvation patterns obtained at the DFT level are verified at the MP2/AVTZ level for $n < 6$. Unlike $HgCl_2$-$(H_2O)_n$ case, where there are at most three Hg-O_w orbital interactions, Cd also establishes four equatorial orbital interactions with water for $n > 6$ leading to a planar square bipyramid hexacoordination around Cd. The first solvation shell is fully attained with 12 water molecules. At the same level of theory the water binding energies are much larger than those previously found for $HgCl_2$ due to the stronger Cd-O_w interactions arising from the smaller core of Cd. For the largest system studied, $CdCl_2$-$(H_2O)_{24}$, both penta- and hexa-coordination stable patterns around Cd are found. However, Born-Opphenheimer molecular dynamics simulations starting from these optimized geometries at 700 K reveal the greater stability of the Cd-pentacoordinated species, where a $CdCl_2$-$(H_2O)_3$ trigonal bipyramid effective solute appears. The Cd-O(water) radial distribution function shows a bimodal distribution with two maxima at 2.4 Å and 4.2 Å, revealing the different coordination spheres, even with such a small number of solvating water molecules.
 [http://dx.doi.org/10.1063/1.4894286]

I. INTRODUCTION

Human activities have contributed to increase heavy metal levels in soil, sediments, and aquatic ecosystems worldwide. Pollution by toxic cadmium and mercury species has become a true environmental problem that plagues nowadays developed and third-world countries. Both metals are well known to be at the root of a plethora of diseases. Although some cadmium-containing products can be recycled, a large share of the general cadmium pollution is caused by dumping and incinerating cadmium-polluted waste.[1] In Europe, for example, cadmium concentration in agricultural soil increases by 0.2% per year. Aquatic cadmium levels have also increased in the last 30 years worldwide and total global emission of cadmium amounts to ∼7000 t/year.[2] Cadmium can have many adverse effects in humans, most notably causing lung, kidney, and testicular damage.[3] Several studies in the last century showed a connection between cadmium intoxication and bone damage, demineralization, and osteoporosis.[4] The most environmentally abundant Cd containing species is $CdCl_2$ (cadmium dichloride) and it has been shown to induce kidney,[5] prostate,[6] and breast cancer.[7] Very recently it has been shown that prenatal exposure to very low levels (10 ppm) of $CdCl_2$ produces persistent changes to thymus and spleen cell phenotypic repertoire as well as the acquired immune response.[8] From the biochemical point of view it is still unclear how $CdCl_2$ enters the cell. The question of passive *vs*. active transmembrane passage for Cd-containing species is dependent on the specific type of ligands bonded to the metal atom. The type of ligands critically determines the bioavailability of these toxic species through the structural and energetic features of these metallic molecules in aqueous environments. Bioavailability is a pivotal issue for Cd toxicity, for the potential for intracellular Cd accumulation and for the biochemical production of organometallic species such metal-hormones and metal-peptide complexes. Several relevant experimental and a few theoretical studies have been reported over the years.[9–13]

One previous theoretical study of relevance here is reported in Ref. 11, where the structures of Group 12 dihalides in their vapor and crystal phases are sought and discussed. The molecular structures of all monomers and dimers (MX2: M = Zn, Cd, Hg, and X = F, Cl, Br, I) were obtained at the DFT-B3PW91 and MP2 levels. Experimentally, the identity and stability of aqueous species formed by cadmium in H_2O–Na/LiCl–HCl–HNO_3 solutions were investigated using X-ray absorption spectroscopy (XANES and EXAFS) with varying chloride concentration, temperature and pH.[10] Results show that aqueous Cd speciation is dominated by the $Cd(H_2O)_6^{2+}$ cation in acidic Cl-free solutions, and by chloride species $CdCl_m(H_2O)_n^{2-m}$ over a wide range of temperatures ($20 \le T \le 450\,^{\circ}C$), acidities ($1 \le pH \le 8$), and chloride concentrations ($0.04 \le mCl \le 18$ mol/kg H_2O). EXAFS spectra from chloride solutions show that with increasing T and mCl the average number of Cl atoms increases from 1 to ∼3 (±0.6), accompanied by a decrease of the number of O from 6 to ∼1 (±0.7), in the nearest coordination sphere around Cd.

At this point we recall also that Ref. 13 recommends a formation constant of $CdCl_2$ is 2.64 which corresponds to a fairly weak interaction between Cd^{2+} and $2Cl^-$ of around −3.6 kcal/mol.

[a]On sabbatical leave from Facultad de Ciencias, Universidad Autónoma del Estado de Morelos, Morelos, Mexico. Electronic mail: alex@uaem.mx.

Another issue related to this problem is the speciation and transformation of the Cd^{2+} in biological environments since, once Cd-containing species cross the cellular membrane, they will chemically interact with one or many complex biological agents. Indeed, if a fully comprehensive biochemical study is to be performed, one must take into account the role of specific enzymes such as metallothionein (MT). MT is a family of cysteine-rich, low molecular weight proteins which are mainly found in the membrane of the Golgi apparatus. MTs have the capacity to bind both physiological (such as zinc, copper, selenium) and xenobiotic (such as cadmium, mercury, silver, arsenic) heavy metals through the thiol group of its cysteine residues, which represents nearly the 30% of its amino acidic residues. MTs function is not completely clear, but experimental data suggest MTs provide protection against metal toxicity (in particular against Cd(II)), that they are involved in the regulation of physiological metals (Zn and Cu) and provide protection against oxidative stress.[14] However, this much more complex issue is clearly out of the scope of the present study.

Another important aspect is the comparison between Cd- and Hg-containing species in solution. Indeed, since Cd and Hg belong to the same group in the periodic table, it is useful to recall what is known about the similar mercury-containing species. Since there are clear parallels to draw between Cd(II) and Hg(II), we highlight recent quantum chemical work on ligand binding free energies and group 12 hydration by the Mercury Science Focus Area at the Oak Ridge National Laboratory.[15] In this context we note that the neutral $HgCl_2$, HgOHCl and $Hg(OH)_2$ species are found to be the most abundant toxic species in aqueous environments.[16,17] Gutknecht[18] addressed the permeability of $HgCl_2$, $HgCl_3^-$, $HgCl_4^{2-}$, $Hg(OH)_2$, and HgClOH through lipid bilayer membranes. This classic study revealed that these membranes are 20 times more permeable to $HgCl_2$ than to water and more than a million times more permeable to $HgCl_2$ than to Na^+, K^+, or Cl^-. In a more recent study similar conclusions were found by Barkay *et al.*[19]

A fundamental question related to the bioavailability issue is whether $HgCl_2$ and $CdCl_2$ can be considered as water-dressed molecules or not during the transmembrane transport process making them available to the cell interior. In this regard we recently addressed the solvation of $HgCl_2$ through a DFT study using stepwise cluster solvation,[20] and through Monte Carlo simulations of the aqueous solution.[21] We found that the hydrogen bond network is crucial to allow orbital-driven interactions between Hg(II) and the water molecules. In order to study $HgCl_2$ in the aqueous phase we performed extensive Monte Carlo (MC) simulations including ∼1000 water molecules and taking into account up to 10^{10} configurations. The MC simulations were done using very refined MP2 derived interaction potentials which are polarizable, flexible, and include non-additive effects. The MC simulations of the solution revealed that $HgCl_2$ behaves like a hydrophobic solute, which explains the rather easy passage of $HgCl_2$ through the cell membrane; these simulations of the solution also showed that one to three water molecules establish Hg-O_w interactions in the fashion of a hydrophilic solute.[21]

In this context some natural questions arise concerning $CdCl_2$: does the aqueous solvation environment of $CdCl_2$ resemble that of $HgCl_2$? Are the water binding energies of $CdCl_2$, both in the gas phase and in the condensed phase, as low as those found for $HgCl_2$?

Since to best of our knowledge no information, theoretical or experimental, concerning these issues is available, we aim at providing answers to these questions. Therefore, we report here some structural and energetic results for the aqueous microsolvation of $CdCl_2$ using cluster models. We shall also address some key structural aspects and the thermal stability of the largest water-solvated systems through Born-Oppenheimer molecular dynamics. As previously done for $HgCl_2$, these cluster results will serve as references for further solvation studies in the condensed liquid phase.[21] Sec. II presents the methodological details, while in Sec. III we present the results and discuss them in the light of previous microsolvation studies of $HgCl_2$. Finally, in Sec. IV we present some conclusions and perspectives.

II. COMPUTATIONAL DETAILS

A. Basis sets and electronic structure methods

A systematic study by stepwise hydration of $CdCl_2$ was carried out at the DFT level, i.e., water molecules were added to previously optimized $CdCl_2$-$(H_2O)_n$ structures for n = 1–24. As it will be shown later, 24 is twice the number of water molecules needed to form the first solvation shell of $CdCl_2$. Incremental water binding free energies and optimized structures have been computed. The core electrons of cadmium were substituted by the small core Stuttgart-Dresden relativistic effective core potentials (RECP) and augmented versions of their associated basis sets.[22,23]

Since Hargittai and Hoffman have shown that the Cd-Cl distance is very well reproduced at the B3PW91 level (2.273 Å *vs.* 2.28 Å exp.) with the cc-pVTZ basis for Cl[10] we used here the same approach. In order to more accurately deal with the molecular flexibility of $CdCl_2$ upon solvaton, the Cd RECP basis set has been augmented by a set of polarization and diffuse even-tempered ($\alpha = 1/3$) functions: 0.0190 and 0.0066 *s* exponents, 0.0012 *p* exponent, 0.075 and 0.025 *d* exponents. As previously done for $HgCl_2$ and $Hg(OH)_2$, the oxygen and hydrogen atoms have been described with the 6-31G** basis sets. Full geometry optimizations were carried out at B3PW91 level without any symmetry restrictions. Analytical frequency calculations were done to verify the stable nature of the stationary points (all minima) and the Gibbs free energies were computed at 298 K within the harmonic approximation. All the calculations were carried out with the Gaussian03 program.[24]

In order to assess the accuracy and reliability of the DFT results, the structures of the $CdCl_2$-$(H_2O)_n$ systems for small n ($n < 6$) were also optimized at the MP2 level using the large *aug-cc-pV(D,T)Z* basis sets for O and H.[25] Thus, optimized geometries at the MP2/AVTZ level and frequency calculations at the MP2/AVDZ level are also reported for these systems. The reliability of the MP2 single reference method was determined by the calculation of the T1Diagnostic at the CCSD/AVDZ level for the $n = 0$, 1, 2, and 3 cases using the

corresponding MP2/AVTZ optimized geometries. As could be expected, in all cases the T1Diagnostic was found to be quite small (T1Diag < 0.0142). These results are in agreement with the previous report by Shepler *et al.*[26] where they used the MP2 and B3LYP methods to study the microsolvation of several mercury-mono and -dihalide species. Thus, as in our previous studies of $HgCl_2$ and $Hg(OH)_2$, the MP2 method also provides reliable structural and energetic references for the $CdCl_2$-$(H_2O)_n$ clusters.

B. DFT molecular dynamics

The thermal stability of the largest cluster studied here, $CdCl_2$-$(H_2O)_{24}$, has been tested using Born-Oppenheimer molecular dynamics (BO-MD) simulations at the B3PW91 level. The simulations were carried out with the Geraldyn2.1 code based on the method developed by Raynaud *et al.*,[27] which uses the velocity-Verlet integration scheme.[28] For the integration of the equations of motion a time step of 0.5 fs was used. A Nosé–Hoover chain of four thermostats[29,30] was used to control the temperature at 700 K during the 10 ps of the simulation. The electronic structure DFT calculations (done with Gaussian09) involve 669 molecular orbitals and the 10 ps BO-MD simulation took 26 CPU days on 32 processors@2.8 GHz running the Linux versions of Geraldyn2.1-Gaussian09.

III. RESULTS AND DISCUSSION

A. The isolated $CdCl_2$ molecule and calibration of the Cd,Cl valence basis sets

For bare $CdCl_2$, at the MP2/RECP(Cd)+cc-pVTZ(Cl) level, the Cd-Cl bond distance is 2.254 Å, to be compared with the experimental value of 2.266 Å.[31,32] We emphasize that the corresponding B3PW91 optimized distance (2.273 Å) is in excellent agreement with these values. Here we note that while the Cl-Hg-Cl angle is 178.6° for bare $HgCl_2$,[33] for $CdCl_2$ the Cl-Cd-Cl angle is perfectly linear. The atomic NPA charges are −0.675 for Cl and +1.35 for Cd. Since the dipole moment of $CdCl_2$ is zero due to its linear geometry, in an aqueous environment it could be expected that $CdCl_2$ interacts roughly as strongly as $HgCl_2$ with the dipole moments of the solvating water molecules. We shall later make this comparison in the context of the water binding energies. We proceed now to address the water-microsolvated species.

B. Geometries of the $CdCl_2$-$(H_2O)_n$ optimized complexes

The interaction of $CdCl_2$ with water was studied *via* stepwise solvation by adding a number (n) of water molecules to the system, with n = 1–24. Special care was taken in order to insure that all the Cl-Cd-Cl–O_w (O_w stands for water oxygens) and Cd-Cl-O_w-O_w dihedral angles were properly sampled with each additional water molecule. The stability of the optimized structures with varying number of water molecules (Figures 1 and 2) was verified by the absence of imaginary frequencies at the MP2 level with the various basis sets used here. A detailed analysis of the geometries of the optimized complexes with one to six water molecules is given in the supplementary material.[43] Note that the optimized structures with three, four, and five water molecules all belong to the C_s point group and their geometries are similar to those obtained for the $HgCl_2$ case.[20] However, a particularly interesting case arises when a seventh water molecule is considered, since two different stable structures are found (Figure 2). The first one is directly related to the optimized hexa-hydrated structure, since the new water molecule does not alter the pentacoordination pattern around Cd. The second, slightly more stable

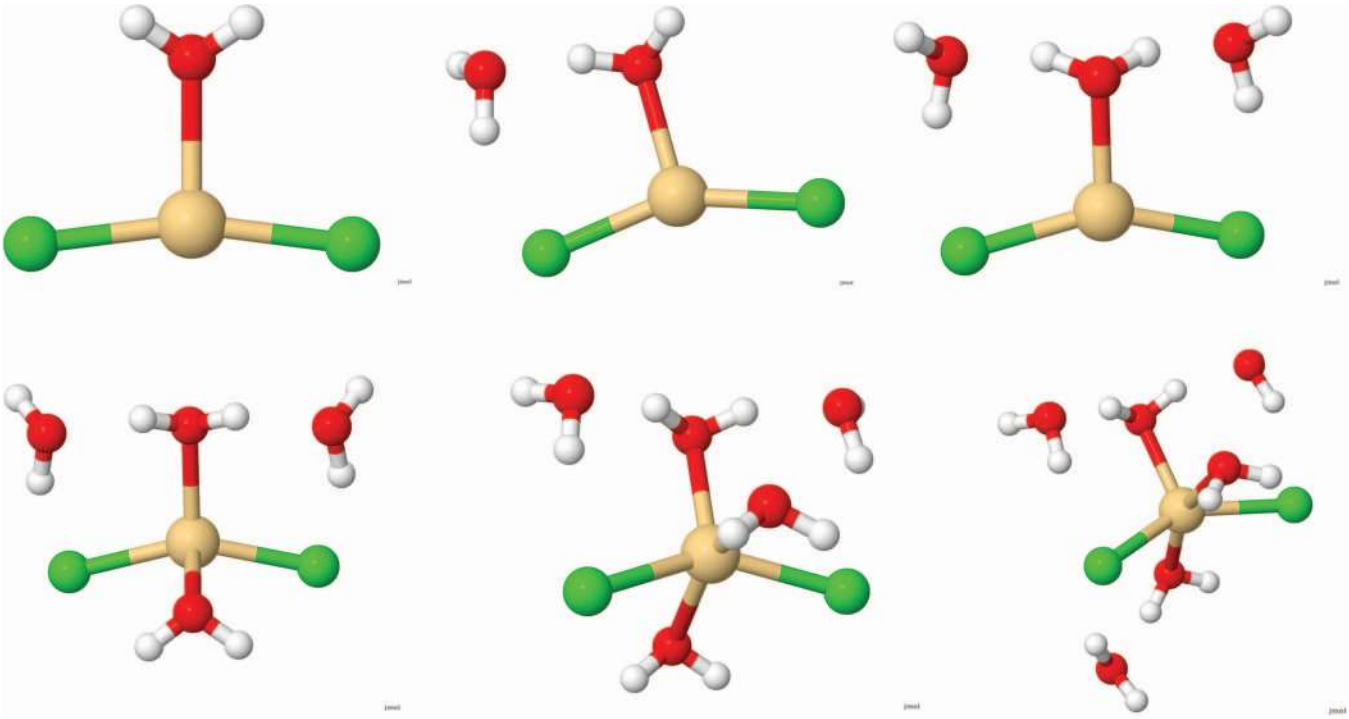

FIG. 1. Optimized geometries of $CdCl_2$ solvated by one to six water molecules.

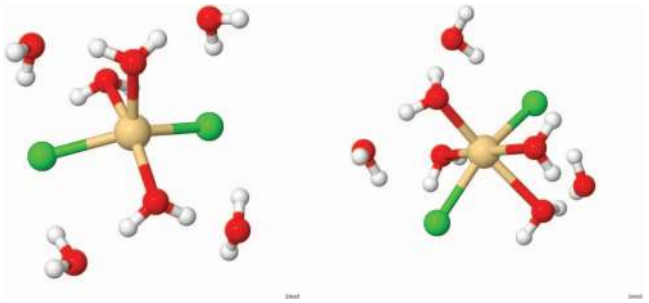

FIG. 2. Two stable geometries of $CdCl_2$ solvated by seven water molecules. The pentacoordinated structure is ($\Delta G^0_{298} = 2.1$ kcal/mol) more stable than the hexacoordinated one. Although stable pentacoordinated structures exist, hexacoordination around Cd was found to be slightly favored with a larger number of water molecules (see text).

structure, leads to a total rearrangement of the coordination around Cd. The incoming water molecule is located in the equatorial plane so that four water oxygens directly interact with the Cd atom and the Cl-Cd-Cl angle increases to 152°. The Gibbs free energy of this square bipyramid hexacoordinated pattern around Cd is only 2 kcal/mol higher than that of the one of the pentacoordinated Cd structure, suggesting thermodynamic equilibrium between these structures at room temperature.

We stress however that two of O_w-Cd-O_w angles (67° and 109°) between these equatorial waters are far from being 90°, as would be the case of a perfect square bipyramid hexacoordinated Cd^{+2} bare ion in water (see Table II). Further stepwise addition of water molecules only leads to the creation of new hydrogen bonds between the water network.

We present in Figure 3 the special case of $n = 12$ where four nearly linear chains composed of three water molecules surround $CdCl_2$. The special feature of this structure is that the 3-water chains are roughly parallel to the Cl-Cd-Cl axis, so that Cd is coordinated by two Cl and four water oxygens. Note that the Cl-Cd-Cl angle goes back to being almost linear at 176°. One Cl atom is surrounded by four H atoms whose Cl-H distances are 2.17, 2.17, 2.58, and 2.76 Å, while the other Cl atom interacts with four (at 2.19, 2.26, 2.27, and 2.33 Å) surrounding H atoms.

This cluster with $n = 12$ defines the first solvation shell of $CdCl_2$ since the addition of another water molecule can only be accomplished by the creation of one or two hydrogen bonds with the existing water network and zero new interactions with the solute atoms. We have explored the stepwise addition of water molecules up to $n = 24$, which is twice the number of molecules needed to build the first solvation shell. As expected, for $n > 12$ the number of possible local minima in the corresponding potential energy surfaces grows due to the increasing number of hydrogen bonding patterns between the incoming water molecules. For instance, in the $n = 17$ case we have found three different structures whose Gibbs free energies differ by 1.2 and 2.6 kcal/mol with respect to the lowest-lying one we report here. For $n = 21$, by modifying the coordination of the hydrogen bond pattern of the water network, four low-energy optimized structures were found that are within 3.6 kcal/mol from the lowest-energy isomer. Therefore, we report here only the lowest energy structure without the assurance that it is the absolute minimum at 0 K in each case. Nevertheless, it should be stressed that all the optimized structures for n > 12 show that the hexacoordination (2Cl, $4O_w$) around Cd is slightly more stable than the pentacoordinated (2Cl, $3O_w$) counterparts. A particular feature found for the optimized structures with $n > 12$ is that the Cl-Cd-Cl angle is larger than 173°, suggesting that the solute recovers its linearity when fully hydrated.

Figure 4 shows the optimized penta- and hexacoordinated structures for the $CdCl_2$-$(H_2O)_{24}$ case. Since this is a cluster-based study, it is clear that our best estimate of the energy difference between the penta and the hexa-coordinated structures corresponds to the system with the largest number of water molecules: for the case with $n = 24$ the hexa-coordinated structure has a Gibbs free energy 5.6 kcal/mol lower than the penta-coordinated Cd at 298 K (−2031.444202 a.u. *vs.* −2031.435146 a.u. at the B3PW91/6-31G** level).

Table I shows the main optimized B3PW91/6-31G** geometrical parameters of gaseous and solvated $CdCl_2$-$(H_2O)_n$ systems. In order to compare this DFT description with *ab initio* results, we present MP2/AVTZ optimized values for the smaller systems (n < 6). The data corresponding to water oxygen atoms (O_w) concern only those directly interacting with Cd.

Analysis of this table leads to the following conclusions concerning the comparison of DFT and MP2 results: (a) the intra-solute DFT Cd-Cl distances are slightly shorter than the MP2 ones; (b) the optimized DFT and MP2 Cl-Cd-Cl angles obtained are very similar for all values of *n*; (c) the shortest Cd-O_w distances are slightly overestimated with respect to the MP2 values; and (d) the Cl-H distances (not shown in Table I)

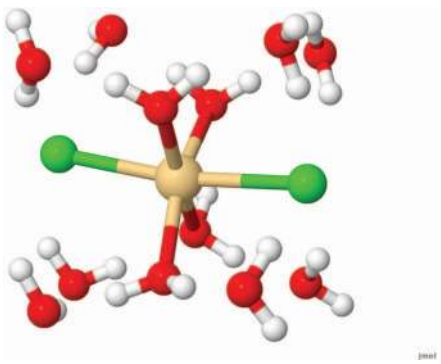

FIG. 3. The optimized structure with 12 water molecules. Note the nearly linear Cl-Cd-Cl (176.6°) angle and the nearly flat O_w-O_w-O_w-O_w (4.8°) dihedral angle of the equatorial waters around Cd.

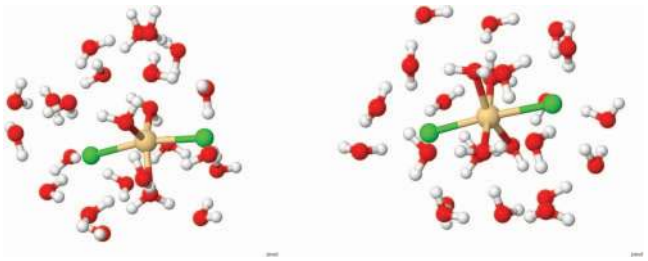

FIG. 4. The optimized penta- and hexacoordinated-Cd structures with 24 water molecules. The Gibbs free energy of the latter is only 5.6 kcal/mol lower than that of the former.

TABLE I. Main optimized B3PW91/6-31G** geometrical parameters of gaseous and solvated $CdCl_2$-$(H_2O)_n$ systems. For comparison MP2/AVTZ optimized values are given in parentheses for small *n*. For n > 12 only data corresponding to the lowest-energy structure are shown. The water oxygen atoms (O_w) are those directly linked to Cd. Distances in Å and angles in degrees. O_w-Cd-O_w are the angles concerning the water oxygens coordinated to Cd.

n	Cd-Cl	Cd-Cl	Cl-Cd-Cl	Cd-O_w	O_w-Cd-O_w
0	2.273 (2.254)	2.273 (2.254)	180.0 (180.0)	...	...
1	2.307 (2.318)	2.307 (2.318)	166.0 (164.8)	2.398 (2.371)	...
2	2.312 (2.322)	2.353 (2.357)	155.3 (155.1)	2.30, 3.80 (2.29, 3.85)	...
3	2.349 (2.356)	2.349 (2.356)	151.6 (150.6)	2.240, 3.67, 3.67 (2.237, 3.72,3.72)	...
4	2.389 (2.394)	2.389 (2.394)	149.2 (147.5)	2.24, 2.42, 3.62, 3.62 (2.25, 2.39, 3.64, 3.64)	99.8 (98.1)
5	2.452 (2.453)	2.452 (2.453)	143.1 (141.3)	2.23, 2.42, 2.46, 3.58(2.24, 2.40, 2.44, 3.59)	94.0, 107.6, 158.3 (90.9, 105.5, 163.5)
6	2.478	2.493	140.4	2.23, 2.33, 2.49, 3.58	90.8, 105.2, 163.1
7-h[a]	2.513	2.521	145.7	2.26, 2.40, 2.51, 2.60	64.6, 88.0 86.6, 120.9
12	2.628	2.824	175.8	2.21, 2.28, 2.38, 2.42,	70.8, 85.3 94.7, 108.5
17	2.618	2.714	176.2	2.31, 2.37, 2.38, 2.40	80.5, 86.3, 88.1, 104.6
21	2.623	2.732	177.1	2.32, 2.35, 2.38, 2.42,	77.2, 86.6, 93.2, 106.4
24-p[a]	2.527	2.692	161.8	2.23, 2.24, 2.32, 3.51	100.3, 116.6, 142.4
24-h[a]	2.619	2.709	178.9	2.29, 2.31, 2.33, 2.42	79.6, 86.7, 87.8, 105.5

[a]Data of the penta(p) or (h) hexacoordinated-Cd structures.

are slightly longer (∼0.1 Å) than those found at the MP2 level. However, beyond the small quantitative differences provided by these two levels of theory, the most important conclusion is that the faster B3PW91/6-31G** approach yields exactly the same coordination patterns found using the considerably more expensive MP2/AVTZ method, for all values of *n*. We recall that the DFT calculations were done using the smaller 6-31G** basis sets for oxygen and hydrogen, which allow the study of much larger systems.

In order to analyze the effect of increasing solvation upon the vibrational modes of the solute we have obtained the vibrational spectra for the isolated molecule as well as for all the $CdCl_2$-$(H_2O)_n$ optimized complexes. More accurate results are presented in the supplementary material[43] at the MP2/AVDZ level of theory for $n < 6$ but exactly the same trends were found at the B3PW91/6-31G** level. Note the presence of three additional normal modes when a new water molecule is added to cluster, one of them appearing around 1600 wavenumbers and two more between 3000 and 4000 cm^{-1}, corresponding to the bending, the symmetric and the antisymmetric stretching modes of the additional water molecule. The vibrational frequencies of the $CdCl_2$ intramolecular modes monotonically decrease with solvation, in agreement with the elongation of the Cd-Cl bonds shown in Table I. In particular, when five water molecules surround $CdCl_2$, the frequencies of the Cl-Cd-Cl stretching (symmetric and antisymmetric) and bending modes decrease by 50, 116, and 15 cm^{-1}, respectively.

C. Continous solvent models

In order to address the possible effects of the polar aqueous medium on the geometry of the optimized structures including explicit water molecules, for selected values of *n* we performed calculations using the Polarizable Continuum Model (PCM) of Tomasi *et al.*[34] and the implicit solvation (SMD) method of Marenich *et al.*[35] as implemented in Gaussian09. Since we addressed continuous solvent effects for large *n* we used the same 6-31G(d,p) (O,H) basis sets as above. In the PCM approach the solvent, in this case water, is represented by a continuous dielectric which is characterized by its dielectric constant ($\varepsilon = 78.355$). Thus, we re-optimized the structures determined as minima *in vacuo* for three values of *n* (5, 12, and 21) using both implicit solvation methods. Table II shows the main geometrical parameters obtained *in vacuo* and their modified values obtained after re-optimization with the PCM and SMD schemes. Figure 5 shows the optimized geometries for n = 12 using both implicit solvation methods.

We find that for these cases the PCM scheme leads to similar optimized geometries as those obtained *in vacuo*, with Cd-Cl and Cd-O_w distances slightly longer (∼0.1 Å) than those obtained *in vacuo*. Note that changes to the Cl-H distances are smaller, except for n = 12. While the coordination patterns around Cd remain unchanged in all cases, the optimized PCM geometry for $n = 5$ is a first order transition state with a low-imaginary frequency of 18 wavenumbers (a figure showing the vectors corresponding to this vibrational mode is given in the supplementary material[43]). While the elongation of Cd-Cl and Cd-O_w distances becomes less pronounced for the largest *n*, it is clear that the PCM scheme favors the separation of the explicit water molecules from the solute, leading to a more loosely bound solvating water network around $CdCl_2$. On the other hand, SMD results are strongly *n*-dependent. While for $n = 5$ and 21 the optimized coordination patterns around $CdCl_2$ remain qualitatively unchanged, for $n = 12$ the SMD optimization leads to a complete rearrangement of the solvation pattern, most remarkably to the dissociation of one of the Cl atoms from the $CdCl_2$ moiety. Since for $n = 21$ the PCM and SMD schemes lead to the same coordination patterns and $n = 12$ case represents the system with the first solvation shell, these results lead us to a more in depth analysis of the $n = 12$ case. We found that the qualitatively different results are due to the specific ways in which these methods deal with the solvation of the "external" water molecules, those which critically define the supermolecular surfaces and cavity volumes used in these implicit solvation schemes. In the case with large *n* ($n = 21$), the "internal" water molecules

TABLE II. Optimized B3PW91 main geometrical parameters (Å) of selected $CdCl_2$-$(H_2O)_n$ structures *in vacuo* and with continuous solvent models. The optimized PCM structure is a first order transition state for $n = 5$ with $\omega = 18i$ cm^{-1}.

n	*In vacuo*	PCM	SMD
5	Cd-Cl: 2.48, 2.48	2.55, 2.55	2.58, 2.58
	Cl-Cd-Cl: 143.3°	146.7°	140.9
	Cd-O_w: 2.23, 2.39, 2.45	2.29, 2.39, 2.51	2.28, 2.38, 2.58
	Cl-H: 2.31, 2.31	2.33, 2.33	2.29, 2.29
12	Cd-Cl: 2.64, 2.79	2.75, 2.99	2.64, 4.71
	Cl-Cd-Cl: 176.6°	160.3°	168.1°
	Cd-O_w: 2.22, 2.28, 2.37, 2.37	2.25, 2.30, 2.39 2.55	2.28, 2.31, 2.33 2.45
	Cl-H: 2.09, 2.39, 2.61;	2.14, 2.24, 3.88;	2.23, 2.30;
	2.15, 2.23, 2.27	2.13, 2.20, 2.28	2.10, 2.14, 2.20
21	Cd-Cl: 2.60, 2.60	2.58, 2.61	2.70, 2.77
	Cl-Cd-Cl: 172.4°	170.2°	160.2°
	Cd-O_w: 2.31, 2.36. 2.38, 2.39	2.31, 2.35, 2.37 2.38	2.33, 2.34, 2.37 2.40
	Cl-H: 2.08, 2.26, 2.40;	2.08, 2.25, 2.38;	2.19, 2.23, 2.27;
	2.18, 2.20, 2.25	2.18, 2.19, 2.26	2.19, 2.20, 2.22

directly interacting with $CdCl_2$ already show hydrogen bonding with "external" second solvation shell waters; therefore the different solvation schemes of these external water molecules do not appreciably affect their bonding pattern with the solute and, thus, the optimized structures are very similar with both methods. However, for the case with only 12 water molecules, we found that, while there is practically no difference in the final optimized cavity surface areas for the 39 exposed spheres (36 from the 12 waters and 3 from the solute) with both methods (405.5 Å^2 with PCM and 409.6 Å^2 with SMD), the 315.4 Å^3 cavity volume with the SMD approach is 25% smaller than that optimized (419.6 Å^3) using the PCM method. This much smaller volume of the SMD-optimized system (Figure 4, right) can clearly be seen when compared to the PCM optimized structure (Figure 4, left) and the minimization of this volume is achieved in SMD by dissociation of one of the Cl moieties from CdCl fragment, so that two water molecules rotate allowing better solvation of the Cl ion while, at the same time, they interact with the remaining water molecules through the hydrogen bond network. This larger cavity volume minimization with SMD is at the root of the different qualitative descriptions obtained with both methods for the $n = 12$ case. Unfortunately, we cannot perform a more detailed energetic analysis since the Gaussian09 code does not yield the values of the electrostatic and non-electrostatic contributions when the PCM approach is applied. For the SMD approach only the non-electrostatic contribution is given; it amounts to +8.87 kcal/mol at the *in vacuo* optimized geometry and it increases to +9.45 kcal/mol at the final optimized continuous solvent geometry.

The important conclusion drawn here is that a considerably larger number of explicit water molecules than those needed to build the first solvation shell must be used in the cluster model in order to obtain reliable results when including the effects of a continuous solvent.

D. Water binding energies

As previously done for the $HgCl_2$-$(H_2O)_n$ case, the water binding energies (WBE) have been obtained as $\Delta G_{298}(n) = G_{298}(CdCl_2\text{-}(H_2O)_n) - G_{298}(CdCl_2) - n\ G_{298}(H_2O)$. At this stage it is interesting to compare these water binding energies with those previously reported for the $HgCl_2$ case.[17] Figure 6 shows the evolution of these energies as function of n for $CdCl_2$ and $HgCl_2$, and we recall that both have been calculated at the B3PW91/6-31G** level of theory. The absolute

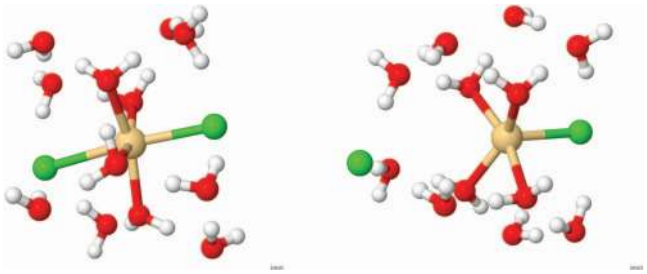

FIG. 5. Optimized $CdCl_2$-$(H_2O)_{12}$ complex with PCM (left) and SMD (right) solvation models. Note the complete Cl dissociation in the latter case (Cd-Cl distance of 4.71 Å).

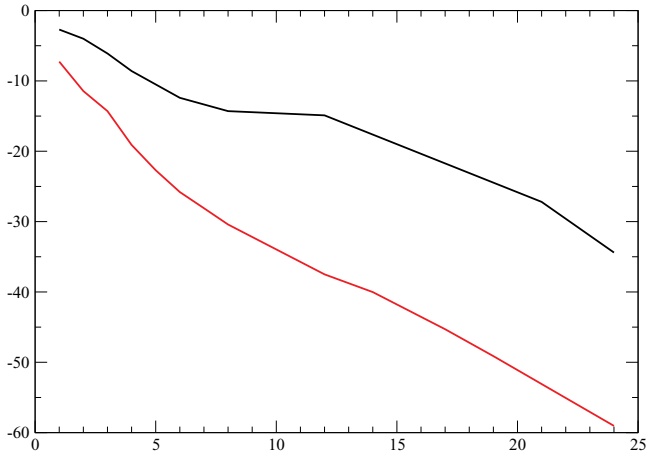

FIG. 6. Gibbs free water binding energies (kcal/mol) at 298 K *vs.* the number of solvating water molecules for $HgCl_2$ (black) and $CdCl_2$ (red). Data for $HgCl_2$-$(H_2O)_n$ taken from Ref. 20.

Gibbs free energies and the WBE are reported in as function of n in the supplementary material.[43] Two interesting facts can be observed from these curves. First, it is clear that the WBE for $CdCl_2$ are nearly twice as large as those found for $HgCl_2$ for all values of n. Note that this ratio is even larger for small values of n, for instance it is −7.4/−2.7 for $n = 1$. This fact stems from the stronger chemical interaction of water with the metal (see below the bonding analysis) due to the much smaller core of Cd *vs*. that of Hg, so that the orbital overlap of the valence orbitals with the lone pairs of oxygen is larger in the former case. Second, note the presence of three regimes for both solutes; each curve has, *grosso modo*, two growth regions (where the slope of the second region is smaller than the slope of the first region) separated by a plateau. Clearly the plateau for $HgCl_2$ is larger, extending from $n = 7$ to $n = 12$. However, the number of water molecules needed to build the first solvation shell around $HgCl_2$ has been estimated around 24,[20] while only 12 molecules are needed in the present case.

At this point it is insightful to assess the energetic changes of the solute due to the microsolvation. This has been achieved by performing a single-point calculation for the solute with the geometry it attains in each microsolvated system. Table III shows the evolution of the total and incremental deformation energies at the B3PW91/6-31G** level as functions of n.

The large geometrical changes (mainly concerning the Cl-Cd-Cl angle) of $CdCl_2$ due to solvation imply important (up to ca. 18 kcal/mol for the heptahydrated system) energetic changes of the solute; however, these positive deformation energies are largely compensated by the attractive orbital interactions that Cd establishes with the water oxygens, up to four in the latter case.

E. Solute-water bonding analysis

The bonding situation in the $CdCl_2$-$(H_2O)_n$ hydrated complexes was studied by means of the Natural Bond Orbital scheme. In particular, knowing that from $n = 7$ an octahedral hexacoordinated Cd is found, we shall use the heptahydrated complex as a representative case of the solute-water bonding. Apart from the polarized covalent bond between Cd and the two Cl, it has been possible to identify four donor-acceptor interactions, i.e., bonds, between four water molecules and the cadmium center, all of them in equatorial positions with respect to the axial Cl atoms. These bonds were found at the second order donor-acceptor NBO analysis and involve donation from an sp^2 lone pair of water and an empty hybrid dp orbital of cadmium (note that more than 40 kcal/mol are gained through these interactions). This is further highlighted by scrutinizing the WIberg Bond Indexes (WBI). Indeed, the polarized covalent Cd-Cl bonds lead to a WBI of 0.38 that is only two-three times larger than those found between the three water molecules and the cadmium atom, whose WBI are 0.19, 0.13, and 0.13. This clearly indicates that the four Cd-OH_2 bonds are relatively strong, in line with the water binding free energy (−35.4 kcal/mol).

Summarizing the results of the NBO analysis for small n: one, one, one, two, and three direct Cd-O_w orbital-driven interactions with water oxygens were found for $n = 1, 2, 3, 4$ and $n = 5$, respectively (schematically depicted as bars joining the Cd and water oxygens in Figures 1–4). Interestingly, for $n = 5$ the situation is qualitatively very different from what was found for the $HgCl_2$-$(H_2O)_5$ complex. Indeed, for the latter only two bonds were found between the water molecules and $HgCl_2$ in the pentahydrated complex; even with six solvating water molecules, the water hydrogen bond network expands but no other Hg–O_w interaction was found.[20] Here we recall that the water binding energies for $HgCl_2$ are much smaller than the ones obtained for $CdCl_2$. Thus, the magnitude of the microsolvation energy is clearly associated with the strength of the bonding interaction between the metal center and the closest water molecules, Cd being more covalent than Hg.

F. DFT Born-Oppenheimer molecular dynamics

To address the role of thermal effects on the largest solvated structure, several of Born–Oppenheimer MD simulations (B3PW91/6-31G**) at 700 K were carried out. As in previous studies,[36,37] the higher than room temperature (700 K in this case) was chosen because it provides a better sampling of the potential energy surface of the system; note that this temperature is higher than the critical point of water but it involves a rather low thermal energy of ∼1.5 kcal/mol.

The BO-MD simulations started either from the $CdCl_2$-$(H_2O)_{24}$ penta- or from the hexacoordinated-Cd optimized structures with random velocities consistent with the fixed temperature. We found that when the simulations started from the hexacoordinated-Cd optimized structure, the geometry of the solvated species quickly became pentacoordinated. Figure 7 shows the evolution of the relevant Cd-O_w distances for two of the simulations starting from the hexacoordinated-Cd structure. Note that the water exclusion from the Cd coordination occurs via two pathways: either one of the equatorial water decoordinates from Cd after a few oscillations to increase the surrounding water network or, two of the equatorial water molecules simultaneously decoordinate from Cd while one of the water molecules of the outer layer becomes coordinated with Cd and remains in the pentacoordination environment throughout the rest of the simulation. At this point we recall that the Gibbs free energy of the hexacoordinated-Cd structure is only 5 kcal/mol lower than

TABLE III. Single-point B3PW91/6-31G** calculation for $CdCl_2$ with the geometry it attains in the microsolvated system. Total energies in a.u. and deformation energies in kcal/mol. Cl-Cd-Cl angle θ in degrees.

	$n = 0$	$n = 1$	$n = 3$	$n = 5$	$n = 7$
E (a.u)	−196.968086	−196.965683	−196.959720	−196.947489	−196.938033
ΔE	0	1.5	5.1	12.4	18.3
θ	180	164.8	150.6	143.1	145.7

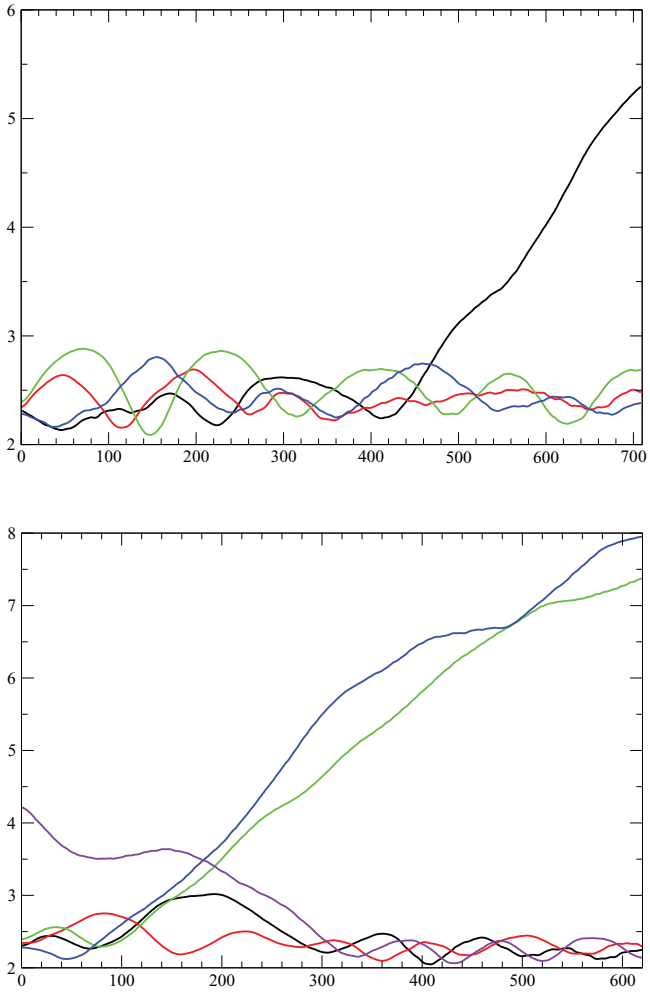

FIG. 7. Time evolution of the shortest Cd-O_w distances (Å) during the simulations starting from the hexacoordinated Cd structure. Horizontal axis in fs.

that of the pentacoordinated-Cd species, so that these simulations reveal the greater dynamic stability of the latter structures at higher temperatures. On the other hand, when the simulation starts from the optimized pentacoordinated-Cd structure the trigonal bipyramid coordination around Cd remained stable throughout the simulation, as shown in Figure 8, with transient formation of octahedric $CdCl_2$-$(H_2O)_4$ complexes; two such structures were observed during the course of this simulation. A particularly important feature of these dynamical results is the stability of the cluster-derived first solvation shell.

In this case the temporal evolution of the shortest Cd-O_w bond distances (Figure 8) indicates that the Cd center is mainly pentacoordinated, although due to finite temperature effects, it becomes hexacoordinated for brief periods of time. We note that the fourth incoming water molecule is also located in the equatorial region. Note also that, during the hexacoordination, no water-exchange was observed as it is the same water molecule that gets into the first coordination sphere and that is expulsed after a few hundredths of femtoseconds. The Cd-O_w radial distribution function (Figure 9) was extracted from this simulation. This plot shows that the solvation sphere is well-defined with two distinct peaks. The

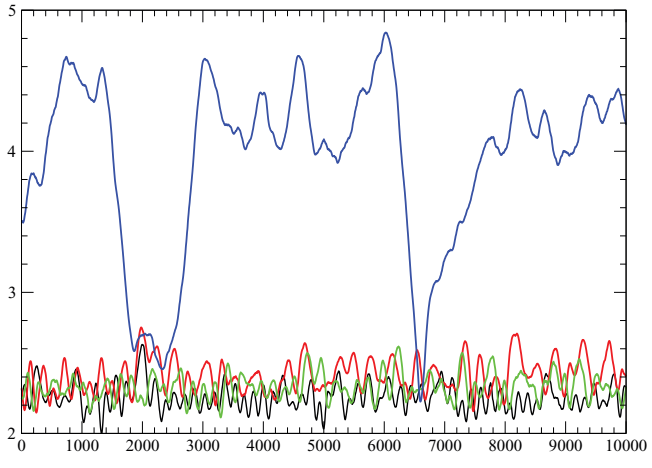

FIG. 8. Evolution of the shortest Cd-O_w distances (Å) during the simulation starting from the optimized pentacoordinated Cd structure. Horizontal axis in fs. Note the transient Cd-hexacoordination.

first one around 2.3–2.4 Å corresponds to the Cl-ligands and to directly Cd-coordinated water molecules whereas the second one (around 4.5 Å) corresponds to the water solvation sphere with a shoulder at 5.5 Å. Interestingly, the first peak corresponds to 1/3 of the second one whereas the shoulder is roughly 2/3 of the highest peak. Thus one can conclude that, on average, only 1/6 of the water molecules lies in the first coordination sphere (that is 4 molecules) whereas 18 water molecules remain in the second coordination shell. The shape of the radial distribution function is in line with very little exchange between the two solvation spheres, at least during the 10 ps of the longest simulation we performed, in line with the analysis of the Cd-O_w bond distance evolution. This is very different from what was reported in the case of $HgCl_2$, where the Hg-O_w radial distribution function revealed no clear structure of the first and second solvation spheres.[18] These results are consistent with a stronger orbital interaction in $CdCl_2$ as pointed out earlier in this study.

Finally we would like to mention that the quasichemical theory (QCT) of Pratt *et al.*[38] provides a new rigorous statistical mechanical framework for the hydration of ions. Recent developments of quasichemical theory provide new

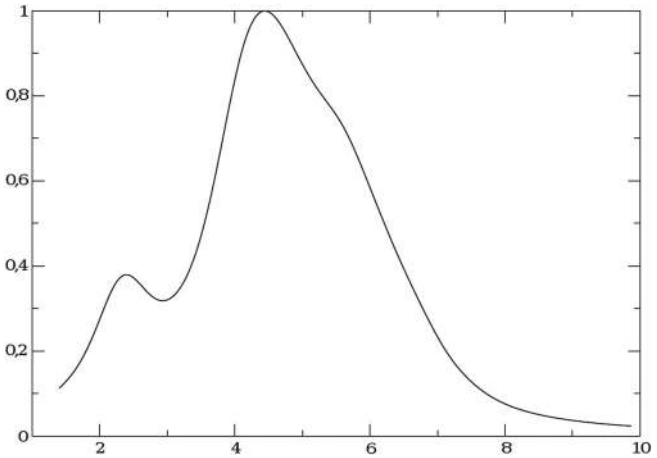

FIG. 9. Cd-O_w radial distribution function extracted from the BO-MD 10 ps simulation of the CdCl2-$(H_2O)_{24}$ cluster. Horizontal axis in Å.

interpretative tools to the theory of solutions from a molecular point of view. While QCT provides a natural organization for calculations of ion-water chemical interactions in the treatment of ion hydration free energies, for non-polar solutes dissolved in liquid water, QCT avoids physical assumptions of the van der Waals perturbative type and thus resolves questions arising from reference system assumptions; in this respect we note that the QCT has been successfully used to describe the hydration energy of CF_4(aq).[39] QCT was originally developed with a sharp cutoff to spatially define the inner shell of the solute providing, therefore, a clear counting scheme of solute-solvent interactions within that shell; however, it has been extended to use soft-cutoffs[40] that have some advantages over the hard-cutoff original version. QCT has been recently applied to study the solvation energy of CO_2 in water.[41] We note that this approach allowed the authors to obtain the most probable number of water molecules around the solute as a function of the inner-shell radius; in this case for varying cutoff radii of 2.7, 3.0, and 3.3 Å, the most probable numbers of water molecules found within these inner shells are 1, 4, and 7.2, respectively. A particularly important result of that report is that the analysis of the free energy components reveals that the weak hydration free energy results from a balance of unfavorable molecular packing and favorable chemical association. Since both CO_2 and $CdCl_2$ are non-polar linear molecules, a similar situation might arise for the latter in liquid water. Therefore, work is in progress to address in detail this aspect applying QCT as well as the Cd-water coordination number using Monte Carlo simulations of the condensed phase with refined *ab initio*-derived potentials.[42]

IV. CONCLUSIONS AND PERSPECTIVES

$CdCl_2$ is the most common cadmium-containing species and it is known to be responsible for a plethora of human health disorders. Aqueous solvation of $CdCl_2$ is crucial in the context of the transmembrane passage of this species into the cellular environment. As a first step in the approach to the aqueous solvation problem of $CdCl_2$, we report a systematic quantum chemical study of the structures, vibrational frequencies and the water binding energies of the $CdCl_2$–$(H_2O)_n$ (n = 1–24) microsolvated species. The hybrid DFT method was calibrated against MP2 energetic and structural results for small n. As previously found for $HgCl_2$,[20] $Hg(OH)_2$,[36] and HgClOH,[37] the hybrid B3PW91 functional was shown to yield reliable water binding energies and optimized structural parameters when combined with the RECP(aug) valence basis for Cd, the cc-pVTZ(Cl), and the 6-31G(d,p) basis sets for O and H. With a small number of solvating water molecules the intramolecular geometry of $CdCl_2$ is significantly modified by the microsolvation environment; in particular, when the solute is pentahaydrated the Cl-Cd-Cl angle sharply decreases to 143°. Nevertheless, the large deformation energies are largely compensated by the attractive orbital interactions of Cd with the lone pairs of the closest solvating water molecules. When seven water molecules solvate $CdCl_2$, two nearly degenerate stable structures were found, one where Cd is pentacoordinated and another where Cd is hexacoordinated, the former being slightly more stable. However, for larger values of n the opposite happens; in particular for n = 24, the hexacoordinated structure is 5 kcal/mol more stable than the pentacoordinated one. As previously mentioned, the $CdCl_2$ formation constant corresponds to only −3.6 kcal/mol (the bulk of which will be in the formation of $CdCl^+$), thus the relative energetics between hexa- and penta-coordination around Cd are related to differences in speciation probabilities consistent with the formation of Cd^{2+}(aq) and $2Cl^-$(aq). The relative stability of the penta/hexacoordinated structures is clearly determined by the specific ways in which the energy gain provided by the inter-water hydrogen bond network is established (in each case with a fixed n) around the $CdCl_2$ molecule *vs.* the energy gain obtained by direct O_w-Cd^{2+} and H-Cl^- interactions; a beautiful example of this fact is found in the case of seven water molecules where the penta-coordinated system has three O_w coordinated to Cd and two water hydrogens coordinated to each Cl; the hexacoordinated species has four Ow coordinated to Cd but one of the Cl is only coordinated to one water hydrogen. This situation where solvation around Cl^- is diminished turns out to be slightly (2.1 kcal/mol) less favorable. As the number of water molecules increases more of them are available to better solvate the Cl^- ions, thus leading to slightly more stable hexa-coordinated Cd structures, but only when the static description is used.

The first solvation shell is shown to consist of 12 water molecules (eight of them not coordinated to Cd), in sharp contrast with the much bulkier $HgCl_2$ case, where ∼24 molecules are needed to fully form the first solvation sphere.[18] Also, for a given number of solvating water molecules, the Gibbs free water binding energies are shown to be nearly twice those found for the $HgCl_2$ molecule.

Geometry optimizations using the PCM and SMD continuous solvent schemes for selected values of n were done. When a small number of explicit water molecules is considered, qualitatively different results (very critically, the Cd-O_w coordination distances and Cl-Cd-O_w angles) appear due to the specific ways in which these methods deal with the solvation of the "external" water molecules, i.e., those which critically define the cavity volumes used in the implicit solvation schemes. The important conclusion drawn is that a considerably larger number of explicit water molecules than that needed to build the first solvation shell must be used in the cluster model in order to obtain reliable results when including the effects of a continuous solvent with both of these schemes.

Several BO molecular dynamics simulations at high temperature of the largest cluster, $CdCl_2$–$(H_2O)_{24}$, were done. An important result is that these BO-MD studies revealed the greater dynamical stability of the pentacoordinated-Cd species as compared with the statically more stable hexacoordinated complex. In sharp contrast with previous results reported for the $HgCl_2$ molecule where no clear water structure around mercury was found, the Cd-O_w radial distribution function reveals a well defined structure around Cd where three to four equatorial water molecules are coordinated around the Cd center.

The Cd-O(water) radial distribution function shows a bimodal distribution with two maxima at 2.4 Å and 4.2 Å, revealing the different coordination spheres, even with such as

small number of solvating water molecules. Our best estimate of the free energy difference between the pentacoordinated-Cd and the statically more stable hexacoordinated-Cd is 5.6 kcal/mol, corresponding to the largest cluster $CdCl_2$-$(H_2O)_{24}$.

However, we stress that the conclusions (especially those concerning the penta vs. hexacoordination around Cd) extracted from these simulations pertain only to gas-phase hydration since the dynamic many-body effects arising from the third and subsequent shells of solvation are missing, therefore, further studies must be done to accurately address the solvation in the liquid medium. The understanding of the solvation of $CdCl_2$ in the condensed aqueous phase requires the use of sophisticated classical Cd(II)-water, Cl-water and $CdCl_2$-water-water non-additive interaction potentials in conjunction with Monte Carlo or molecular dynamics simulations for the solution.

As a by-product of the present study, we have obtained reference potential energy surfaces (PES) for this microsolvated molecule and the corresponding harmonic vibrational frequencies with one to five water molecules at a high level of theory (MP2/AVTZ). These PES, which already include many-body non-additive effects, will be used to develop very accurate MDCHO classical interatomic potentials needed to perform the Monte Carlo (MC) simulations of the solvation in the aqueous condensed phase, as recently done for $HgCl_2$.[21]

In particular when we consider the full liquid solvation we wish to answer if, as we found for $HgCl_2$, there exists an $CdCl_2$–$(H_2O)_k$ effective solute, what is the number k and what are its symmetry properties, i.e., the local coordination environment of the Cd atom in the liquid phase. Our final goal will be to study the structural and energetic properties of $CdCl_2$ in the condensed liquid phase through classical MC simulations and applying the quasi-chemical theory of Pratt *et al.* using refined *ab initio* derived interaction potentials.

ACKNOWLEDGMENTS

The authors thank support from the ECOS-ANUIES/CONACYT Mexican-French cooperation program through project M10-P01. A.R.-S. also thanks support from CONACYT basic science Project No. 130931 and from the CONACYT Sabbatical program. This work was partially supported by Programme Investissements d'Avenir under the program ANR-11-IDEX-0002-02, reference ANR-10-LABX-0037-NEXT. L.M. thanks CINES and CALMIP as well as the Humboldt Foundation. We thank the reviewers for their helpful comments and suggestions, in particular for pointing out the possible application of QCT to this complex problem in further studies.

[1] L. Jarup, Br. Med. Bull. **68**, 167 (2003).
[2] M. Stoeppler, "Cadmium," in *Metals and Their Compounds in the Environment*, edited by E. M. Weinheim (Verlag Chemie, 1991), pp. 805–849.
[3] G. F. Nordberg, Biometals **17**, 485 (2004); O. Barbier, G. Jacquillet, M. Tauc, M. Cougnon, and P. Poujeol, Nephron Physiol. **99**, p105 (2005).
[4] K. Nogawa, E. Kobayashi, Y. Okubo, and Y. Suwazono, Biometals **17**, 581 (2004); G. Kazantzis, *ibid.* **17**, 493 (2004).
[5] A. Hartwig, Met. Ions Life Sci. **11**, 491 (2013), and references therein.
[6] P. Aimola, M. Carmignani, A. R. Volpe, A. DiBendetto, L. Claudio, M. P. Waalkes, A. van Bokhoven, E. J. Tokar, and P. P. Claudio, PLoS One **7**, e33647 (2012).
[7] E. Ponce, PLoS One **8**, e72639 (2013).
[8] I. Holásková, M. Elliott, M. L. Hanson, and R. Schafer, Toxicol. Appl. Pharmacol. **265**, 181 (2012).
[9] B. C. Shepler and K. A. Peterson, J. Phys. Chem. A **110**, 12321 (2006).
[10] K. J. Donald, D. Hargittai, and R. Hoffmann, Chem. – Eur. J. **15**, 158 (2009).
[11] E. F. Bazarkina, G. S. Pokrovski, A. V. Zotov, and J. L. Hazeman, Chem. Geol. **276**, 1 (2010).
[12] P. Butterworth, I. H. Hillier, N. A. Burton, D. J. Vaughan, M. F. Guest, and J. A. Tossel, J. Phys. Chem. **96**, 6494 (1992).
[13] K. J. Powell, P. L. Brown, R. H. Byrne, H. Robert, T. Gajda, G. Hefter, A. K. Leuz, S. Sjoberg, and H. Wanner, Pure Appl. Chem. **83**, 1163 (2011).
[14] See, for instance, P. Coyle, J. C. Philcox, L. C. Carey, and A. M. Rofe, Cell. Mol. Life Sci. **59**, 627 (2002).
[15] The Oak Ridge National Laboratory Science Focus Area focuses on the biogeochemical transformations that govern mercury speciation at the sediment-water interface and, particularly, the processes controlling the production of methyl mercury, see http://www.esd.ornl.gov/programs/rsfa/index.shtml. For instance, a study of mercury methylation by novel microorganisms from new environments can be found in C. C. Gilmour, M. Podar, A. L. Bullock, A. M. Graham, S. D. Brown, A. C. Somenahally, A. Johs, R. A. Hurt, Jr., K. L. Bailey, and D. A. Elias, Environ. Sci. Technol. **47**, 11810 (2013).
[16] F. M. M. Morel, A. M. L. Krapiel, and M. Amyot, Annu. Rev. Ecol. Syst. **29**, 543 (1998).
[17] C. Larose, A. Dommergue, M. De Angelis, D. Cossa, B. Averty, N. Marusczak, N. Soumis, D. Schneider, and C. Ferrari, Geochim. Cosmochim. Acta **74**, 6263 (2010).
[18] J. Gutknecht, J. Membr. Biol. **61**, 61 (1981).
[19] T. Barkay, M. Gillman, and R. R. Turner, Appl. Environ. Microbiol. **63**, 4267 (1997).
[20] L. Castro, A. Dommergue, A. Renard, C. Ferrari, A. Ramírez-Solís, and L. Maron, Phys. Chem. Chem. Phys. **13**, 16772 (2011).
[21] J. Hernández-Cobos, A. Ramírez-Solís, L. Maron, and I. Ortega-Blake, J. Chem. Phys. **136**, 014502 (2012).
[22] A. Bergner, M. Dolg, W. Kuechle, H. Stoll, and H. Preuss, Mol. Phys. **80**, 1431 (1993).
[23] W. Kuechle, M. Dolg, H. Stoll, and H. Preuss, Mol. Phys. **74**, 1245 (1991).
[24] M. J. Frisch, G. W. Trucks, H. B. Schlegel *et al.*, Gaussian 09, Revision A.01, Gaussian, Inc., Pittsburgh, PA, 2009.
[25] T. H. Dunning, J. Chem. Phys. **90**, 1007 (1989).
[26] B. C. Shepler, A. D. Wright, N. B. Balabanov, and K. A. Peterson, J. Phys. Chem. A **111**, 11342 (2007).
[27] C. Raynaud, L. Maron, J. P. Daudey, and F. Jolibois, Phys. Chem. Chem. Phys. **6**, 4226 (2004).
[28] L. Verlet, Phys. Rev. **159**, 98 (1967).
[29] S. Nosé, J. Chem. Phys. **81**, 511 (1984).
[30] W. G. Hoover, Phys. Rev. A **31**, 1695 (1985).
[31] M. Hargittai, Chem. Rev. **100**, 2233 (2000).
[32] T. Yokoyama, K. Kobayashi, T. Ohta, and A. Ugawa, Phys. Rev. B. **53**, 6111 (1996).
[33] A. Ramírez-Solís and L. Maron, Int. J. Quantum Chem. **112**, 3484 (2012).
[34] J. Tomasi, R. Cammi, B. Mennucci, C. Cappelli, and S. Corni, Phys. Chem. Chem. Phys. **4**, 5697 (2002).
[35] A. V. Marenich, C. J. Cramer, and D. G. Truhlar, J. Phys. Chem. B **113**, 6378 (2009).
[36] J. I. Amaro-Estrada, L. Maron, and A. Ramírez-Solís, J. Phys. Chem. A **117**, 9069 (2013).
[37] J. I. Amaro-Estrada, L. Maron, and A. Ramírez-Solís, Phys. Chem. Chem. Phys. **16**, 8455 (2014).
[38] L. R. Pratt, R. A. LaViolette, M. A. Gomez, and M. E. Gentile, J. Phys. Chem. B **105**, 11662 (2001).
[39] D. Asthagiri, H. Ashbaugh, A. Piryatinski, M. Paulaitis, and L. Pratt, J. Am. Chem. Soc. **129**, 10133 (2007).
[40] S. Chempath, L. R. Pratt, and M. E. Paulaitis, J. Chem. Phys. **130**, 054113 (2009).
[41] D. Jiao and S. B. Rempe, J. Chem. Phys. **134**, 224506 (2011).
[42] J. I. Amaro-Estrada, J. Hernández-Cobos, and A. Ramírez-Solís, "Coordination numbers in water solvated $CdCl_2$" (unpublished).
[43] See supplementary material at http://dx.doi.org/10.1063/1.4894286 for details of optimized structures and vibrational modes.